ANALYTICA CHIMICA ACTA 613 (2008) 163–168

available at www.sciencedirect.com

ScienceDirect

journal homepage: www.elsevier.com/locate/aca

Label-free aptasensor for platelet-derived growth factor (PDGF) protein

*Tesfaye Hailu Degefa, Juhyoun Kwak**

Department of Chemistry, Korea Advanced Institute of Science and Technology (KAIST), Daejeon 305-701, Republic of Korea

ARTICLE INFO

Article history:
Received 24 January 2008
Received in revised form
3 March 2008
Accepted 5 March 2008
Published on line 14 March 2008

Keywords:
Aptamer
Target protein
Label-free
Aptasensor

ABSTRACT

A label-free aptasensor for platelet-derived growth factor (PDGF) protein is reported. The aptasensor uses mixed self-assembled monolayers (SAMs) composed of a thiol-modified PDGF binding aptamer and 6-mercaptohexanol (MCH) on a gold electrode. The SAMs were characterized by cyclic voltammetry (CV), electrochemical impedance spectroscopy (EIS), and differential pulse voltammetry (DPV) before and after binding of the protein using $[Fe(CN)_6]^{3-/4-}$, a redox marker ion as an indicator for the formation of a protein–aptamer complex. The CVs at the PDGF modified electrode showed significant differences, such as changes in the peak currents and peak-to-peak separation, before and after binding of the target protein. The EIS spectra, in the form of Nyquist plots, were analyzed with a Randles circuit while the electron transfer resistance R_{ct} was used to monitor the binding of the target protein. The results showed that, without any modification to the aptamer, the target protein can be recognized effectively at the PDGF binding aptamer SAMs at the electrode surface. Control experiments using non-binding oligonucleotides assembled at the electrode surfaces also confirmed the results and showed that there was no formation of an aptamer–protein complex. The DPV signal at the aptamer functionalized electrode showed a linearly decreased marker ion peak current in a protein concentrations range of 1–40 nM. Thus, label-free detection of PDGF protein at an aptamer modified electrode has been demonstrated.

1. Introduction

The detection and quantification of proteins play essential roles in fundamental research as well as in clinical practice. Recently, there has been increasing interest in protein sensing based on SAMs of aptamers [1,2]. Aptamers are single-stranded DNA or RNA molecules, isolated from large pools of random sequence oligonucleotides that are capable of binding with small molecules (cocaine, adenosine, and potassium) [3–5], and biological entities such as proteins [6–9] and cells [10] with high affinity and specificity. In addition to remarkable target diversity and tight-binding capability, aptamers offer ease of synthesis and stability such as longer shelf-life, making them ideal alternative candidates for molecular recognition elements in a wide range of bioassays as well as in the development of protein arrays [11,12].

Platelet-derived growth factor (PDGF) is a protein that regulates cell growth and division. However, a survey of the literature shows there have been only a few reports on sensing of this important protein. PDGF protein sensing using fluorescence [13–19], nanoparticles [20,21], and electrochemistry [22,23] has been reported. The reported methods involve either labeling of the aptamer with a reporter or the use of an aptamer–primer complex as part of the sensing element.

* *Corresponding author*. Tel.: +82 42 869 2833; fax: +82 42 869 2810.
E-mail address: Juhyoun_Kwak@kaist.ac.kr (J. Kwak).
0003-2670/$ – see front matter © 2008 Elsevier B.V. All rights reserved.
doi:10.1016/j.aca.2008.03.010

Table 1 – The aptamer and control sequence of oligonucleotide strands[a]

Name	Sequence
The PDGF aptamer	5′-Thiol(C6)-CAG GCT ACG GCA CGT AGA GCA TCA CCA TGA TCC TG-3′
Oligo-I	5′-Thiol(C6)-CAG CGT ACG GCA CGT ACC GAT TCA CCA TGA AGC TG-3
Oligo-II	5′-Thiol(C6)-GCA GTA ACA AGA ATA AAA CGC CAC TGC-3′

[a] The aptamer sequence and the oligonucleotides sequence are adapted from literature [15,27].

Meanwhile, label-free protein sensors have attracted considerable attention in recent years [2]. In this approach, the aptamer is assembled on an electrode surface as a sensing layer and the changes in the interface before and after binding of the protein allow protein sensing. In the absence of a target protein, the aptamer, which acts as a sensing layer is in a dynamic condition and does not significantly affect the electron transfer from redox marker ions, such as $[Fe(CN)_6]^{3-/4-}$, to the electrode. Once the target protein binds to the aptamer, the aptamer shows a conformational switching and will adopt a tertiary structure [24]. This change usually leads to an increased repulsive (steric and electrostatic) interaction between the aptamer–protein complex and the marker ions. This approach has been used by our group [25] and other groups [6,8] to develop label-free aptasensors for thrombin, a critical enzyme in blood clotting. However, to date, no work on the label-free detection of PDGF protein has been reported. Thus, in this paper we extend the approach described above to a PDGF protein. Electrochemical methods such as cyclic voltammetry (CV) and electrochemical impedance spectroscopy (EIS) were used to monitor the influence of the protein–aptamer complex on the current response and the charge transfer impeded at the interface, respectively, in the presence of the redox marker ions $[Fe(CN)_6]^{3-/4-}$. Furthermore, differential pulse votammetry (DPV) was also carried out to investigate the linear range.

2. Experimental

2.1. Chemicals and reagents

Unless otherwise indicated, all chemicals were obtained from Sigma or Aldrich (Yongin, Korea). Recombinant human PDGF-BB, bovine serum albumin (BSA), and lysozyme were provided by Sigma (Yongin, Korea). The aptamer and the oligonucleotides (see Table 1) employed in this work were synthesized and HPLC purified by Genotech (Daejeon, Korea). The aptamer and the control oligonucleotides were dissolved in 10 mM phosphate buffer (pH 7) containing 5 mM $MgCl_2$.

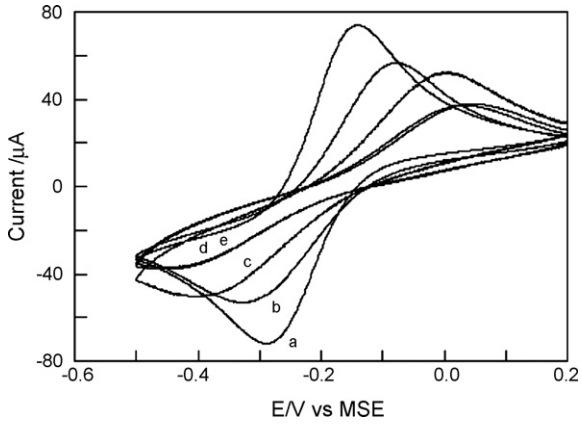

Fig. 2 – CVs of 1 mM $[Fe(CN)_6]^{3-/4-}$ (1:1) at PDGF aptamer modified Au electrode before (a) and after (b–e) formation of aptamer–protein complex: (a) 0, (b) 1, (c) 10, (d) 20 and (e) 100 nM of target protein.

2.2. Electrochemical measurements

Cyclic voltammetry was performed using AUTOLAB 10 (Eco Chemie, Netherlands) interfaced with a personal computer. A standard three-electrode cell was used with either aptamer or oligonucleotides SAMs modified gold plate as a working electrode, $Hg|HgSO_4|K_2SO_4$ (sat) electrode (MSE) as a reference electrode, and a Pt wire counter electrode. Unless otherwise indicated, all cyclic voltammetry measurements were recorded at a scan rate of 50 mV s^{-1}. Using the frequency response analyzer (FRA) of AUTOLAB 10, the impedance spectra at a bias potential of −0.2 V (vs. MSE), which was superimposed on 5 mV rms sinusoidal potential modulations, were measured for 30 frequencies from 50 mHz to 2 kHz. The data are represented in Nyquist plots (Z″ vs. Z′, Z″ = imaginary part of impedance and Z′ = real part of impedance). The respective semicircle diameter corresponds to the charge-transfer resistance, R_{ct}, the values of which are calculated

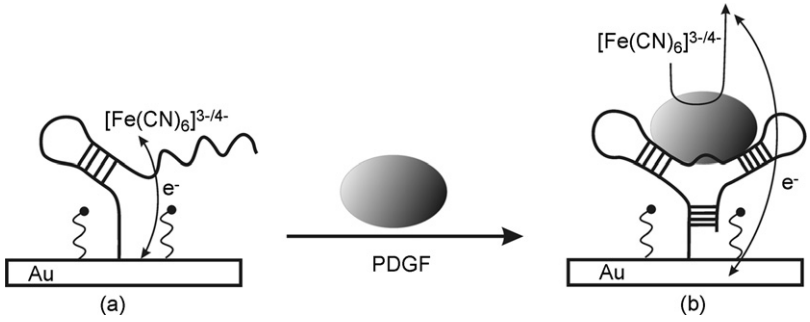

Fig. 1 – Label-free electrochemical sensing of PDGF protein using PDGF binding aptamer self-assembled monolayers (SAMs) on a gold electrode and electrochemical transduction (a) before and (b) after target protein recognition.

using the fitting program of AUTOLAB 10 (FRA, version 4.9 Eco Chemie, The Netherlands). The impedance spectra are fitted to a Randles equivalent electrical circuit for the aptamer or oligonucleotides modified electrode with/without the target protein, including the solution resistance, R_s, a constant phase element (CPE), the charge-transfer resistance, R_{ct}, and the Warburg impedance, Z_w. From the regression, the charge-transfer resistance R_{ct} is obtained. For the DPV measurements, a modulation amplitude of 0.05 V, a step potential of 0.001 V, and a scan rate of 0.002 V s^{-1} were used. All electrochemical measurements were carried out in 10 mM PB (pH 7.4) containing 0.1 M KCl as a supporting electrolyte.

2.3. *Electrode preparation*

Gold electrodes were prepared by electron-beam evaporation of 40 nm of Ti followed by 150 nm of Au onto Si (1 0 0) wafers. The electrode was cleaned in piranha solution (3:7 (v/v) 30% H_2O_2/70% H_2SO_4), followed by copious rinsing with distilled water (warning: the piranha solution reacts violently with organics). It was then dried with nitrogen gas. The aptamer or the control oligonucleotide modified electrode was prepared by immersing a clean gold substrate in 1 μM aptamer or control oligonucleotide solution for 1 h, followed by rinsing with phosphate buffer. To avoid unspecific binding [26], the aptamer modified electrode was immersed in a 1 mM mercaptohexanol (MCH) solution for 1 h and finally rinsed with the phosphate buffer. The electrode was then dried under stream of nitrogen and ready for use. The resulting monolayer-functionalized electrode was allowed to interact with the protein analyte. The detection strategy is outlined in Fig. 1.

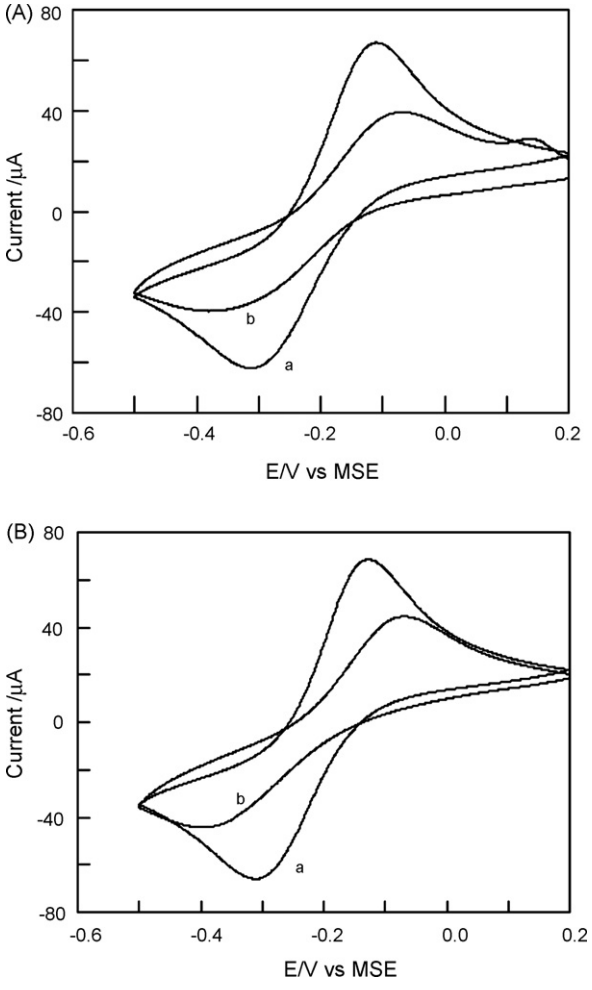

Fig. 3 – CVs of 1 mM $[Fe(CN)_6]^{3-/4-}$ (1:1) at (A) Oligo-I and (B) Oligo-II modified Au electrodes before (a) and after (b) formation of aptamer–protein complex: (a) 0 and (b) 100 nM of target protein.

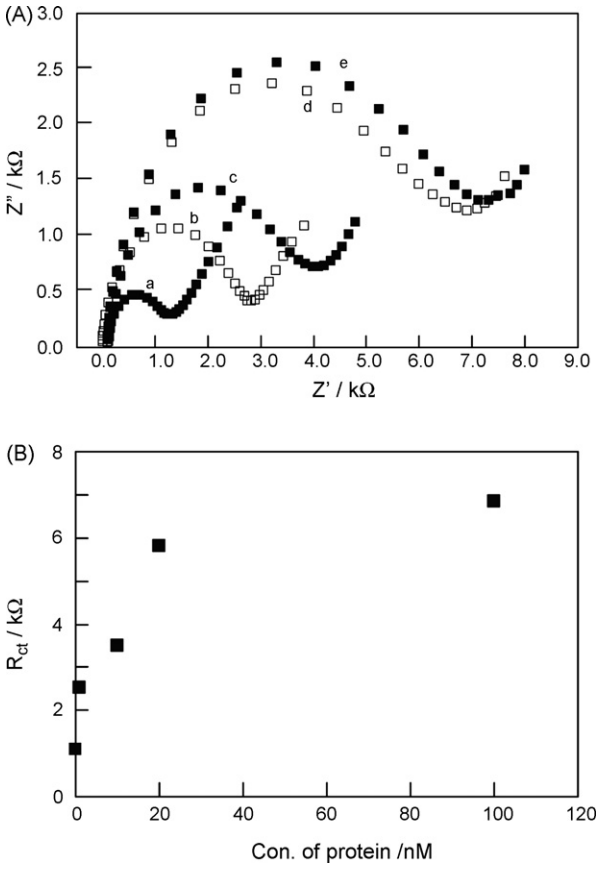

Fig. 4 – (A) Impedance spectra of 1 mM $[Fe(CN)_6]^{3-/4-}$ (1:1) at PDGF aptamer modified Au electrode before (a) and after (b–e) formation of aptamer–protein complex: (a) 0, (b) 1, (c) 10, (d) 20 and (e) 100 nM of target protein. (B) Plot of the electron transfer resistance (R_{ct}) with the concentration of the protein from plots in (A).

3. Results and discussion

The PDGF binding aptamer self-assembled monolayers (SAMs) on the gold surface were characterized by cyclic voltammetry using $[Fe(CN)_6]^{3-/4-}$ as electroactive marker ions. As shown in Fig. 2, a quasi-reversible redox cycle with peak-to-peak separation of 200 mV was observed. This peak-to-peak separation is larger than that observed at the unmodified gold surface, which shows a characteristic reversible redox cycle with a peak-to-peak separation of 80 mV [27]. These changes are attributed to the presence of the aptamer SAMs on the electrode surface. The peak-to-peak separation is fur-

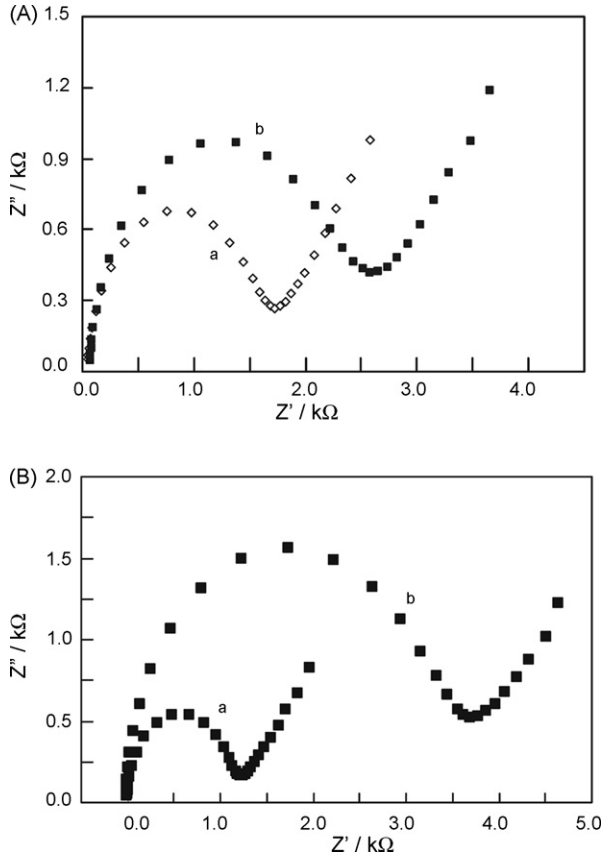

Fig. 5 – Impedance spectra of 1 mM $[Fe(CN)_6]^{3-/4-}$ (1:1) at (A) Oligo-I and (B) Oligo-II modified Au electrodes before (a) and after (b) interacting with the target protein: (a) 0 and (b) 100 nM of protein.

ther increased and the peak current is significantly reduced with increased target protein binding. These observations are in agreement with reports on thrombin binding aptamers assembled on an electrode surface [6,8,25]. The effect has been attributed to a conformational change from a dynamic state to compact structure upon binding of the target protein, allowing and blocking electron transfer between the redox marker ions $[Fe(CN)_6]^{3-/4-}$ and the electrode surface, respectively.

In control experiments, other oligonucleotides (Oligo-I and Oligo-II) were also self-assembled on gold surfaces. Oligo-I has a sequence that is 75% identical to the PDGF binding aptamer. Oligo-II is known to form a closed loop structure but does not bind protein [15,28]. The reduced peak current and increase in peak-to-peak separation observed at the SAMs of Oligo-I and Oligo-II for 100 nM of the target protein are much less than that of the PDGF aptamer (Fig. 3). This is presumably attributable to non-specific binding, as the PDGF protein (pI 9.5–10) possesses some positively charged domains at the experimental conditions (pH 7.4). This would allow electrostatic binding at the oligonucleotides [29].

The above sets of experiments indicate that the PDGF aptamer assembled on the surface possesses inherent specificity to recognize the target protein. The change observed for the PDGF aptamer before and after binding of the target protein is attributed to a conformational switch induced upon binding of the protein [24]. Thus, in the absence of the target protein, the aptamer in its dynamic state allows efficient electron transfer between the redox ions and the electrode surface. However, the electron transfer is significantly affected after target protein binding.

As electrochemical impedance spectroscopy provides more prolific information on the interfacial changes induced from biomolecular interactions at electrode surfaces [30–33], we also studied the modification step and recognition event based on the electron transfer resistances in the presence of the redox couple $[Fe(CN)_6]^{4-/3-}$, measured by electrochemical impedance spectroscopy. Fig. 4A shows the electrochemical impedance spectra (Nyquist plots, Z'' vs. Z'; Z'' = imaginary part of impedance and Z' = real part of impedance) for the PDGF aptamer modified electrode exposed to different concentrations of the target protein. Each spectrum is composed of a semicircular part in a high frequency region and a linear part in a low frequency region, corresponding to the electron transfer process and the diffusion process, respectively.

The spectra were modeled with a Randles equivalent circuit consisting of the solution resistance (R_s), charge-transfer resistance (R_{ct}), constant phase element (CPE), and Warburg impedance (Z_w) [34,35]. The diameter of the semicircle represents the charge-transfer resistance (R_{ct}) at the electrode surface. As shown in Fig. 4A, the diameter of the semicircle increases as the concentration of the target protein is

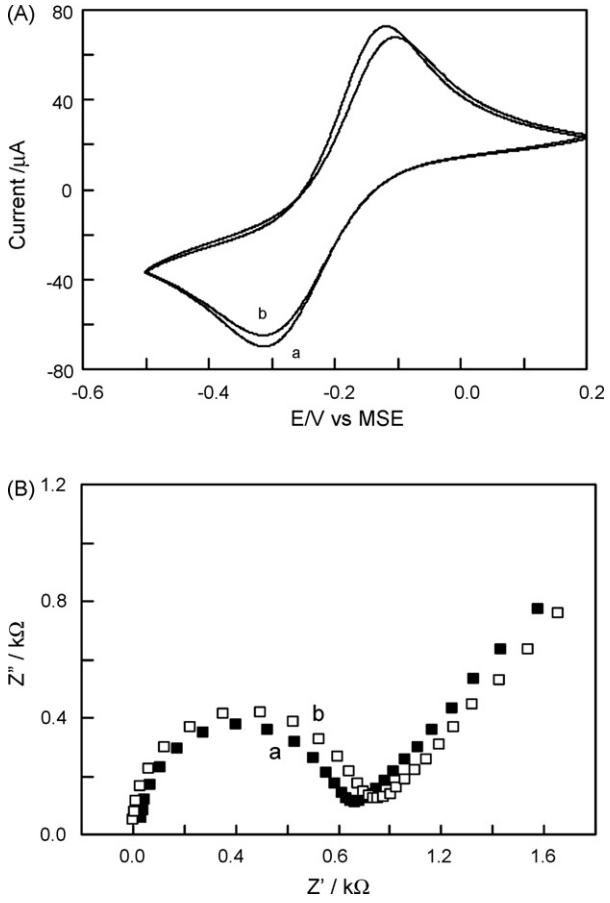

Fig. 6 – (A) CVs and (B) Impedance spectra of 1 mM $[Fe(CN)_6]^{3-/4-}$ (1:1) at PDGF aptamer modified Au electrode before (a) and after (b) addition of 100 nM BSA.

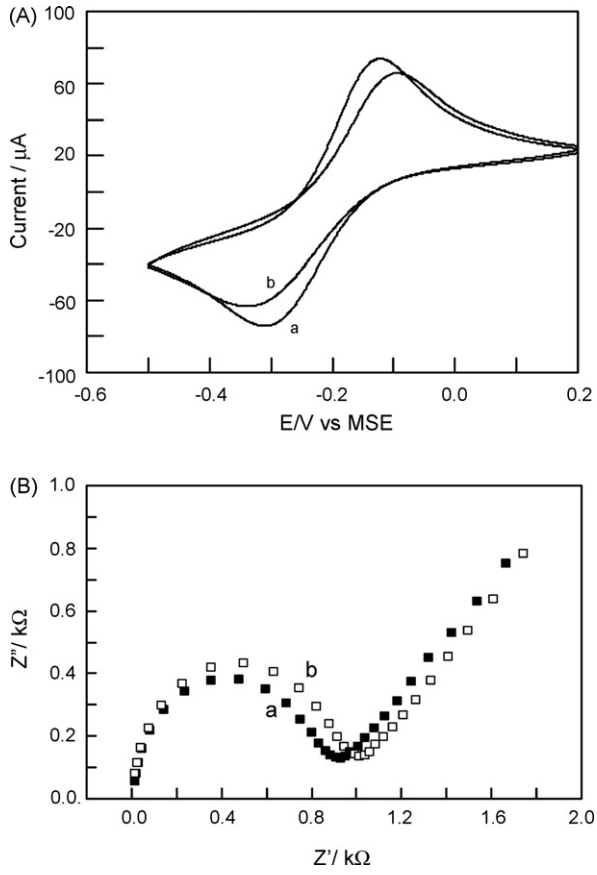

Fig. 7 – (A) CVs and (B) Impedance spectra of 1 mM $[Fe(CN)_6]^{3-/4-}$ (1:1) at PDGF aptamer modified Au electrode before (a) and after (b) addition of 100 nM lysozyme.

increased. This change is attributed to the formation of several compactly packed, tight structures of the aptamer–protein complex upon binding the protein. Thus, the aptamer shows a conformational change from a dynamic to a compact structure [24]. Thus, the repulsive (steric and electrostatic) interactions between the redox marker ions and the electrode surface impede the charge transfer through the interface. The charge-transfer resistance, R_{ct}, increased until all the accessable aptamers were binded by the target protein. A plateau value was achieved at higher protein concentration indicating that no more binding sites are available for formation of the aptamer–protein complex (Fig. 4B).

As control experiments, we have also studied the EIS of the Oligo-I and Oligo-II modified electrode at high concentrations of the target protein (100 nM is considered). The charge-transfer resistance, R_{ct}, observed at a large target protein concentration, is far lower than the charge-transfer resistance, R_{ct}, observed at the PDGF modified electrode (Fig. 5). This was observed directly from the diameter of the semicircle part of the spectra. The lower R_{ct} indicates that both Oligo-I and Oligo-II do not recognize the target protein. The observed increase in R_{ct} in the presence of the protein over that without protein may be attributed to an electrostatic interaction between the aptamer and the protein, which possesses a positively charged domain under the experimental conditions [29].

In additional experiments conducted to confirm that the PDGF aptamer immobilized on the surface recognized the target protein, bovine serum albumin (p*I* 4.8) and lysozyme (p*I* 11.35) were also studied. The selected proteins have p*I* ranges encompassing the p*I* of the target PDGF protein. Thus, the selected protein will have different surface charges at the experimental conditions [29,36]. As can be seen from Figs. 6 and 7, for both proteins, no obvious changes occur in the CV and impedance response, indicating that the binding affinity/specificity between the aptamer and the target protein determines the charge transfer resistance impeded through the interface. Thus, these control experiments show that the surface immobilized PDGF aptamer effectively recognizes the PDGF protein.

After confirming that the PDGF binding aptamer SAMs effectively bind the target protein by using CV and EIS we used DPV to characterize the sensing of the target protein at the aptamer modified electrode surface. As shown in Fig. 8, the DPV current was found to decrease with increased concentration of the target protein. This observation was consistent with the observation that the binding of more protein decreases

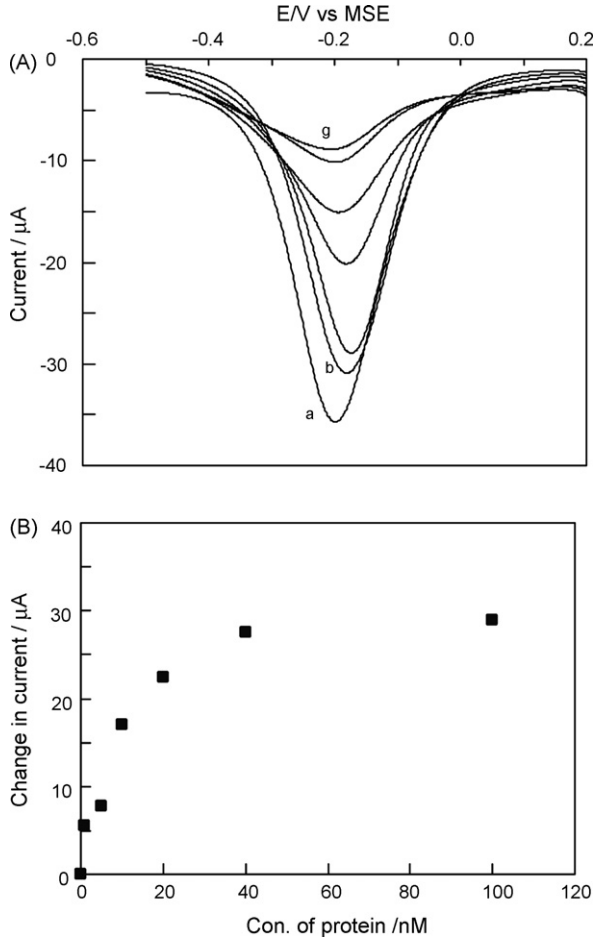

Fig. 8 – (A) DPVs of 1 mM $[Fe(CN)_6]^{3-/4-}$ (1:1) at PDGF aptamer modified Au electrode before (a) and after (b–g) formation of aptamer–protein complex: (a) 0, (b) 1, (c) 5, (d) 10, (e) 20, (f) 40 and (g) 100 nM of target protein. (B) Plot of the changes in the DPVs current as a function of the concentration of the protein from plots in (A).

the access of the marker ions and results in a decrease in the DPV current. The plot of the change in the DPV current with the concentration of the target protein showed a fairly linear increase for the lower protein concentration (<40 nM), after which a plateau was reached at higher protein concentration.

4. Conclusion

In the present study, we have described the sensing of PDGF protein using a mixed self-assembled monolayers (SAMs) of thiolated PDGF binding aptamer and mercaptohexanol on a gold electrode. The immobilized aptamer retains its bioactivity as a sensing layer and allows the target protein recognition event to be transduced electrochemically using cyclic voltammetry, electrochemical impedance spectroscopy (EIS), and differential pulse voltammetry in the presence of a redox couple in solution. Thus, label-free detection and quantification of PDGF protein without the need to label the target protein or labeling of the aptamer have been demonstrated. The previously reported aptasensors for the PDGF protein [13–23] involve the use of fluorescent signaling, electroactive-label or nanoparticles as part of the sensing element. However, the reported method does not involve the use of any of these. Thus, it very simple and attractive.

Acknowledgements

This work was supported by the Korea Science and Engineering Foundation (KOSEF) grant funded by the Korea government (MOST) through the Bioelectronics Program (M10536000001-06N3600-00110) and the Basic Research Program (R01-2005-000-10503-0).

REFERENCES

[1] D.H.J. Bunka, P.G. Stockley, Nat. Rev. Microbiol. 4 (2006) 588.
[2] I. Willner, M. Zayats, Angew. Chem. Int. Ed. 46 (2007) 6408.
[3] B.R. Baker, R.Y. Lai, M.S. Wood, E.H. Doctor, A.J. Heeger, K.W. Plaxco, J. Am. Chem. Soc. 128 (2006) 3138.
[4] A.E. Radi, C.K. O'Sullivan, Chem. Commun. (2006) 3432.
[5] M. Zayats, Y. Huang, R. Gill, C.A. Ma, I. Willner, J. Am. Chem. Soc. 128 (2006) 13666.
[6] H. Cai, T.M.H. Lee, I.M. Hsing, Sens. Actuators B 114 (2006) 433.
[7] F. Le Floch, H.A. Ho, M. Leclerc, Anal. Chem. 78 (2006) 4727.
[8] A.E. Radi, J.L.A. Sanchez, E. Baldrich, C.K. O'Sullivan, Anal. Chem. 77 (2005) 6320.
[9] A.E. Radi, J.L.A. Sanchez, E. Baldrich, C.K. O'Sullivan, J. Am. Chem. Soc. 128 (2006) 117.
[10] D.H. Shangguan, Z.H.C. Cao, Y. Li, W.H. Tan, Clin. Chem. 53 (2007) 1153.
[11] C.L.A. Hamula, J.W. Guthrie, H.Q. Zhang, X.F. Li, X.C. Le, Trends Anal. Chem. 25 (2006) 681.
[12] J.F. Lee, G.M. Stovall, A.D. Ellington, Curr. Opin. Chem. Biol. 10 (2006) 282.
[13] L.T. Yang, C.W. Fung, E.J. Cho, A.D. Ellington, Anal. Chem. 79 (2007) 3320.
[14] X.H. Fang, Z.H. Cao, T. Beck, W.H. Tan, Anal. Chem. 73 (2001) 5752.
[15] X.H. Fang, A. Sen, M. Vicens, W.H. Tan, ChemBioChem 4 (2003) 829.
[16] M.C. Vicens, A. Sen, A. Vanderlaan, T.J. Drake, W.H. Tan, ChemBioChem 6 (2005) 900.
[17] C.J. Yang, S. Jockusch, M. Vicens, N.J. Turro, W.H. Tan, Proc. Natl. Acad. Sci. U.S.A. 102 (2005) 17278.
[18] C.S. Zhou, Y.X. Jiang, S. Hou, B.C. Ma, X.H. Fang, M.L. Li, Anal. Bioanal. Chem. 384 (2006) 1175.
[19] Y.X. Jiang, X.H. Fang, C.L. Bai, Anal. Chem. 76 (2004) 5230.
[20] C.C. Huang, Y.F. Huang, Z.H. Cao, W.H. Tan, H.T. Chang, Anal. Chem. 77 (2005) 5735.
[21] C.C. Huang, S.H. Chiu, Y.F. Huang, H.T. Chang, Anal. Chem. 79 (2007) 4798.
[22] R.Y. Lai, K.W. Plaxco, A.J. Heeger, Anal. Chem. 79 (2007) 229.
[23] L. Zhou, L. Ou, G. Shen, R. Yu, Anal. Chem. 79 (2007) 7492.
[24] J. Wang, Z.H. Cao, Y.X. Jiang, C.S. Zhou, X.H. Fang, W.H. Tan, IUBMB Life 57 (2005) 123.
[25] J.A. Lee, S. Hwang, J. Kwak, S.I. Park, S.S. Lee, K.-C. Lee, Sens. Actuators B 129 (2008) 372.
[26] T.M. Herne, M.J. Tarlov, J. Am. Chem. Soc. 119 (1997) 8916.
[27] T.H. Degefa, J. Kwak, J. Electroanal. Chem. 612 (2008) 37.
[28] R.Y. Lai, E.T. Lagally, S.H. Lee, H.T. Soh, K.W. Plaxco, A.J. Heeger, Proc. Natl. Acad. Sci. U.S.A. 103 (2006) 4017.
[29] P. Schon, T.H. Degefa, S. Asaftei, W. Meyer, L. Walder, J. Am. Chem. Soc. 127 (2005) 11486.
[30] L. Alfonta, A. Bardea, O. Khersonsky, E. Katz, I. Willner, Biosens. Bioelectron. 16 (2001) 675.
[31] A. Bardea, F. Patolsky, A. Dagan, I. Willner, Chem. Commun. (1999) 21.
[32] F. Patolsky, A. Lichtenstein, I. Willner, J. Am. Chem. Soc. 123 (2001) 5194.
[33] J.S. Daniels, N. Pourmand, Electroanalysis 19 (2007) 1239.
[34] A.J. Bard, L.R. Faulkner, Electrochemical Methods; Fundamentals and Applications, Wiley, New York, 2001.
[35] S.M. Park, J.S. Yoo, Anal. Chem. 75 (2003) 455a.
[36] L. Stryer, Biochemistry, W.H. Freeman, New York, 1995.